

Spontaneous emission rate of an excited atom placed near a nanofiber

V.V.Klimov

*P.N.Lebedev Physical Institute, Russian Academy of Sciences, 53 Leninsky
Prospect, Moscow, 117924, Russia
E-mail: klimov@rim.phys.msu.su*

M.Ducloy

*Laboratoire de Physique des Lasers, UMR CNRS 7538
Institut Galilee, Universite Paris-Nord,
Avenue J-B. Clement F 93430
Villetaneuse, France*

Abstract

The spontaneous decay rates of an excited atom placed near a dielectric cylinder are investigated. A special attention is paid to the case when the cylinder radius is small in comparison with radiation wavelength (nanofiber or photonic wire). In this case, the analytical expressions of the transition rates for different orientations of dipole are derived. It is shown that the main contribution to decay rates is due to quasistatic interaction of atom dipole momentum with nanofiber and the contributions of guided modes are exponentially small. On the contrary, in the case when the radius of fiber is only slightly less than radiation wavelength, the influence of guided modes can be substantial. The results obtained are compared with the case of dielectric nanospheroid and ideally conducting wire.

I. INTRODUCTION

At first sight, spontaneous emission is pure atomic process. However as it was first pointed out by Purcell [1], a resonant cavity can change the decay rate substantially. At present it is known that not only resonant cavities but also any material body can influence the decay rate of spontaneous emission [2]. Moreover, the control of decay rate of spontaneous emission already is widely used in practice when making the new efficient sources of the light [3].

In spite of qualitative understanding of influence of material bodies on the spontaneous radiation of atom, only the influence of plane or spherical interface on decay rate is elaborated in detail [4-10].

However the influence of dielectric fiber or metallic wire on decay rate of a single atom is interesting from a theoretical as well as practical point of view. This is due to the fact

that the charged wires are successfully used to control atom motion [11,12]. The cylindrical geometry is also important for investigation of fluorescence of substances in submicron capillaries [13,14]. Very important application of theory of decay rate in presence of dielectric fiber is photonic wire lasers [15,16]. Finally, cylindrical geometry appears naturally when considering carbon nanotubes [17,18]

The influence of ideally conducting cylindrical surface on decay rates is well investigated both for atom inside a cylindrical cavity [19-21] and near cylinder [22].

The spontaneous emission of an atom in presence of a dielectric, semiconductor or metallic cylinder is more complicated process. First investigation of the decay rate of an atom placed on the axis of dielectric fiber was undertaken within classical approach in [23-24]. Recently this problem attracted new interest [25-28]. In [29-30] spontaneous emission near carbon nanotubes was considered. The general line of novel papers was to use numerical methods from the beginning. Unfortunately such an approach cannot answer many qualitative questions. In this paper, we re-investigate the influence of a dielectric cylindrical surface on rates of dipole transitions, using analytical approach. To obtain clear analytical results we will investigate fiber with radius small in comparison with wavelength. We will pay special attention to separate decay rates into radiating and guided (lasing) modes, and nonradiative (lossy) decay rates.

The structure of the rest of the paper is as follows. In Sect. 2 we consider the decay rates for an atom placed in close vicinity to nanofiber with any complex dielectric permittivity, when one can use quasistatic approximations. We obtain simple analytical expression for radiative and nonradiative decay rates for any orientation of dipole momentum of atom. In Sect. 3 we consider the full electrodynamics problem of dipole decay rate near nanofiber with any complex dielectric permittivity. We build the analytical expression for decay rate through contour integral in complex plane of longitudinal wave number. Then we transform general contour integrals to separate contributions of guided and radiating modes. In Sect. 4 general expressions obtained in Sect.3 are applied to z and φ , ρ orientations of dipole momentum of an atom placed on the surface of lossless fiber. In section 5 we present graphical illustrations and discuss the results obtained. Geometry of the problem under investigation is shown in Fig.1.

II. QUASISTATIC ANALYSIS OF DECAY RATE NEAR NANOFIBER

When the distance between the atom and fiber, and the radius of fiber are substantially less than radiation wavelength, the fiber is polarized only near the atom.

As a result, the radiation of atom + fiber system will be of the dipole-type and the relative radiative decay rate will take the following form:

$$\frac{\gamma}{\gamma_0} = \frac{|\mathbf{d}_{tot}|^2}{|\mathbf{d}_0|^2} \quad (1)$$

Here γ_0 is the free space decay rate, \mathbf{d}_{tot} is the total dipole momentum of the atom + nanofiber system and \mathbf{d}_0 is the dipole momentum of atom in free space. The total dipole momentum \mathbf{d}_{tot} can be found from the solution of quasistatic problem

$$\begin{aligned} \text{rot} \mathbf{E} &= 0 \\ \text{div} \mathbf{D} &= 4\pi\rho \end{aligned} \quad (2)$$

where the charge density at the point \mathbf{r} is derived from the dipole momentum of atom

$$\begin{aligned} \rho &= -(d_0 \nabla) \delta^{(3)}(\mathbf{r} - \mathbf{r}') e^{-i\omega t} \\ j &= -i\omega d_0 \delta^{(3)}(\mathbf{r} - \mathbf{r}') e^{-i\omega t} \end{aligned} \quad (3)$$

$\delta^{(3)}(\mathbf{r})$ is the three-dimensional Dirac delta function and ∇' means gradient over radius vector of the atom, \mathbf{r}' . Hereafter we will omit the time dependence of the fields. The continuity conditions for the tangential components of \mathbf{E} and the normal components of \mathbf{D} on the surface of cylinder with dielectric constant ε should be provided as well.

Introducing a potential $\tilde{\varphi}$ by

$$\mathbf{E} = -\nabla (\mathbf{d}_0 \nabla') \tilde{\varphi}(\mathbf{r}, \mathbf{r}'), \quad (4)$$

we obtain, instead of (2) the Poisson equation,

$$\begin{cases} -\nabla^2 \tilde{\varphi} = 4\pi \delta^{(3)}(\mathbf{r} - \mathbf{r}'), & \text{outside cylinder} \\ -\nabla^2 \tilde{\varphi} = 0, & \text{inside cylinder} \end{cases} \quad (5)$$

It is convenient to represent the solution of problem (5) in the form

$$\begin{cases} \tilde{\varphi} = \tilde{\varphi}_0 + \tilde{\varphi}_2, & \text{outside cylinder} \\ \tilde{\varphi} = \tilde{\varphi}_1, & \text{inside cylinder} \end{cases} \quad (6)$$

where φ_0 is the free-space potential given by

$$\tilde{\varphi}_0 = \frac{1}{|\mathbf{r} - \mathbf{r}'|} \quad (7)$$

This free space Green function can be expanded in cylindrical coordinates system (ρ, φ, z) (Fig.1) in the following series [31]:

$$\frac{1}{|\mathbf{r} - \mathbf{r}'|} = \frac{2}{\pi} \sum_{m=0}^{\infty} (2 - \delta_{m,0}) \cos m(\varphi - \varphi') \int_0^{\infty} dh \cos h(z - z') K_m(h\rho') I_m(h\rho) \quad (\rho < \rho') \quad (8)$$

where $\delta_{m,0}$ is Kronecker symbol, K and I are modified Bessel functions [32].

Using this expansion we can find expressions for $\tilde{\varphi}_1$ and $\tilde{\varphi}_2$ by usual mode matching. For potential outside fiber we have the following expression ($\rho > \rho'$)

$$\tilde{\varphi}_2 = \frac{2}{\pi} \sum_{m=0}^{\infty} (2 - \delta_m^0) \cos m(\varphi - \varphi') \int_0^{\infty} dh \cos h(z - z') K_m(h\rho') K_m(h\rho) G_m(ha) \quad (9)$$

where reflection coefficients G_m look as follows:

$$G_m(s) = \frac{(\varepsilon - 1) \frac{dI_m(s)}{ds} I_m(s)}{\frac{dK_m(s)}{ds} I_m(s) - \varepsilon \frac{dI_m(s)}{ds} K_m(s)} \quad (10)$$

It is important to note that for negative values of dielectric constant, $\varepsilon < -1$ (metals), the denominator of (10) is equal to zero for some values of integration variable h . It means that under such conditions, plasmon resonances of the fiber do occur in the system.

To determine the total dipole momentum of the system one should find the asymptotic value of (9) at large distances, $\rho, z \rightarrow \infty$. In the dielectric case ($\varepsilon > 1$) the main contribution to (9) is due to $m=1$ term and has the form

$$\tilde{\varphi}_2^{as} = -\frac{\varepsilon - 1}{\varepsilon + 1} \frac{a^2}{\rho'} \cos(\varphi - \varphi') \frac{\rho}{(\rho^2 + z^2)^{3/2}} \quad (11)$$

Comparing the electric potential of reflected field

$$\tilde{\varphi}_2^{dip} = (\mathbf{d}_0 \nabla') \tilde{\varphi}_2^{as} \quad (12)$$

with dipole potential

$$\tilde{\varphi}_{dip} = \frac{\mathbf{d}_{tot} \mathbf{r}}{r^3} \quad (13)$$

one can find the dipole momentum of fiber, δd . In the case of ρ -orientation of dipole momentum we have

$$\delta d_\rho = d_0 \frac{\varepsilon - 1}{\varepsilon + 1} \frac{a^2}{\rho^2} \quad (14)$$

while in the case of φ orientation the dipole momentum of fiber will be

$$\delta d_\varphi = -d_0 \frac{\varepsilon - 1}{\varepsilon + 1} \frac{a^2}{\rho^2} \quad (15)$$

In the case of z orientation the dipole momentum induced in fiber is equal to zero.

Now combining the dipole momenta of nanofiber and atom and substituting the result in (1) we obtain the radiative decay rates for an atom near nanofiber

$$\begin{aligned} \left(\frac{\gamma}{\gamma_0} \right)_\rho &= \left| 1 + \frac{\varepsilon - 1}{\varepsilon + 1} \frac{a^2}{\rho^2} \right|^2 \\ \left(\frac{\gamma}{\gamma_0} \right)_\varphi &= \left| 1 - \frac{\varepsilon - 1}{\varepsilon + 1} \frac{a^2}{\rho^2} \right|^2 \\ \left(\frac{\gamma}{\gamma_0} \right)_z &= 1 \end{aligned} \quad (16)$$

In the case of atom placed on the surface of fiber these results agree with those obtained in the case of infinitely thin dielectric nanospheroid [33,34]. Besides, these results agree with decay rates of an atom placed on the axis of dielectric fiber [23,24]. Indeed, for $\rho' = a$ we have [from (16)]

$$\left(\frac{\gamma}{\gamma_0} \right)_\rho = \left| \frac{2\varepsilon}{\varepsilon + 1} \right|^2, \quad \left(\frac{\gamma}{\gamma_0} \right)_\varphi = \left| \frac{2}{\varepsilon + 1} \right|^2, \quad \left(\frac{\gamma}{\gamma_0} \right)_z = 1 \quad (17)$$

while for the atom on the axis of nanofiber one has [23,24].

$$\left(\frac{\gamma}{\gamma_0}\right)_\rho = \left(\frac{\gamma}{\gamma_0}\right)_\varphi = \left|\frac{2}{\varepsilon + 1}\right|^2, \quad \left(\frac{\gamma}{\gamma_0}\right)_z = 1 \quad (18)$$

The only difference is for ρ - oriented dipole, where we have enhancement by ε^2 . The physical interpretation is as follows. From QED point of view, decay rate is due to interaction of the dipole with electromagnetic modes, modified by fiber. The tangential (φ, z) components of mode electric field are continuous. So the decay rates of dipoles with (φ, z) orientations on the surface and in the body of fiber should be the same. On the contrary the ρ - component of mode electric field is discontinuous at the surface (The normal component of $D = \varepsilon E$ is continuous). It explains the difference between decay rates of dipole with ρ orientation.

We should also mention that our results do not agree with decay rates of an atom inside photonic wire found in [15,16]. We believe that results [15,16] are misleading because of very crude approximation of fiber by plane waveguide.

In the case of nanowires, that is in the case of $\varepsilon < 0$, the excitation of plasmon resonances is possible and one should add additional terms to (16). The detailed investigation of influence of plasmon resonances to decay rates will be presented elsewhere [35].

Analogous additional terms occur in the case of dielectric fibers also and are due to guided modes. In next sections we will show that these terms are exponentially small for nanofibers. As a result one can use quasistatic formulae for nanofiber safely.

The results obtained, (16), are valid only for dielectric and metallic nanocylinders. The situation is dramatically changed in the case of ideal conductor ($|\varepsilon| \rightarrow \infty$), when reflection coefficients become equal to

$$G_m^{ideal\ conductor}(s) = -\frac{I_m(s)}{K_m(s)} \quad (19)$$

and main contribution to far field is due to $m=0$ term. As a result the potential of reflected field for ρ -orientation of dipole decreases at infinity more slowly than (13). It means that dipole momentum, induced in ideally conducting nanowire, tends to infinity when wire radius goes to zero. Respectively, the decay rate tends to infinity too. This fact is in agreement with the exact solution of the electrodynamics problem [22], where it was shown that the decay rate of radially oriented dipole tends to infinity when cylinder radius tends to zero.

Up to now we considered only the radiative decay rates. However even for dielectric nanobodies the nonradiative losses can be substantial. Here the nonradiative losses are due losses inside nanobody, which are proportional to imaginary part of dielectric permittivity. To take the nonradiative losses into account, one should calculate either the energy flow into nanobody or the full work made by reflected field over dipole. In this case the total decay rates can be described by well-known expression, [36],

$$\frac{\gamma}{\gamma_0} = 1 + \frac{3}{2} Im \frac{\mathbf{d}_0 \mathbf{E}^{(R)}(\mathbf{r}')}{d_0^2 k^3 \sqrt{\varepsilon}} \quad (20)$$

which is valid within classical as well quantum theory for any complex value of dielectric permittivity [37-39]. In (20) $k = \omega/c$ is wavevector.

In the case of bodies (nanobodies) whose size is small in comparison with the radiation wavelength, it is possible to build the perturbation theory in terms of the wave vector \mathbf{k} [40], or, more exactly, in terms of the ratio between the characteristic size a of the body and the wavelength λ , i. e., $ka \ll 1$.

In this case, it is possible to expand the expression for the reflected field $\mathbf{d}_0 \mathbf{E}^{(R)}(\mathbf{r}', \omega)$ governing the change of the decay rate in a power series of k :

$$\frac{\mathbf{d}_0 \mathbf{E}^{(R)}(\mathbf{r}', \omega)}{d_0^2} = a_1 + b_1 k + c_1 k^2 + i d_1 k^3 + \dots \quad (21)$$

where the coefficients a_1 , b_1 , c_1 , and d_1 are determined by solving some quasistatic problems [40]. The coefficient a_1 is determined by solving the static problem on the dipole near the nanobody. It is important to note that the first three terms are due to near fields, while radiation fields appear only starting with the fourth term, which is proportional to k^3 .

In our case, the quasistatic solution is given by

$$\mathbf{E}^{(R)} = -\nabla (\mathbf{d}_0 \nabla') \tilde{\varphi}^{(2)}(\mathbf{r}, \mathbf{r}'), \quad (22)$$

where $\tilde{\varphi}^{(2)}(\mathbf{r}, \mathbf{r}')$ is given by (9). Substituting this expression into (20) and keeping only the leading term in k we obtain the expressions for the nonradiative decay rates near nanofiber:

$$\begin{aligned} \left(\frac{\gamma}{\gamma_0} \right)_\rho^{nonradiative} &= -\frac{3}{\pi k^3} \sum_{m=0}^{\infty} (2 - \delta_{m,0}) \int_0^\infty dh h^2 K_m'^2(h\rho') \operatorname{Im}(G_m(ha)) \\ \left(\frac{\gamma}{\gamma_0} \right)_\varphi^{nonradiative} &= -\frac{6}{\pi k^3} \sum_{m=0}^{\infty} \frac{m^2}{\rho'^2} \int_0^\infty dh K_m^2(h\rho') \operatorname{Im}(G_m(ha)) \\ \left(\frac{\gamma}{\gamma_0} \right)_z^{nonradiative} &= -\frac{3}{\pi k^3} \sum_{m=0}^{\infty} (2 - \delta_{m,0}) \int_0^\infty dh h^2 K_m^2(h\rho') \operatorname{Im}(G_m(ha)) \end{aligned} \quad (23)$$

If the atom is placed in close vicinity to surface of nanofiber ($\rho' \rightarrow a$), these expressions can be reduced to

$$\begin{aligned} \left(\frac{\gamma}{\gamma_0} \right)_\rho &= \operatorname{Im} \left(\frac{\varepsilon - 1}{\varepsilon + 1} \right) \frac{3}{16k^3 (\rho' - a)^3} \\ \left(\frac{\gamma}{\gamma_0} \right)_\varphi &= \left(\frac{\gamma}{\gamma_0} \right)_z = \operatorname{Im} \left(\frac{\varepsilon - 1}{\varepsilon + 1} \right) \frac{3}{32k^3 (\rho' - a)^3} \end{aligned} \quad (24)$$

It should be noted, these expressions are similar to plane dielectric interface, where the reflected field can be described by image dipoles. Comparing (24) and (16) one can see that for usual dielectrics with low losses (for fused silica $\operatorname{Im}\varepsilon \sim 10^{-9}$) nonradiative losses are very small for any reasonable distances of atom from surface. However, when atom is placed exactly on the surface, the nonradiative losses can be enhanced substantially.

III. FULL ELECTRODYNAMICS APPROACH TO DECAY RATES NEAR DIELECTRIC FIBER.

In previous section the decay rates were found within quasistatic approximation without taking into account guided modes or plasmon resonances. In present section within full

Maxwell's propagation theory, we will find the exact expressions for decay rates, which include the contributions from guided modes.

According to [37-39] classical and quantum-electrodynamics calculations give the same results for dipole transition rate normalized to its vacuum value. In present section we shall investigate the influence of a dielectric cylinder on transition rates within classical approach, where the full decay rate can be expressed through classical reflected field at the atom position (20). Thus the reflected field must be found to determine the total decay rate. To find the reflected field, it is necessary to solve the full system of Maxwell's equations where dipole momentum of oscillator is a source and use appropriate boundary conditions.

To find the reflected field we follow the approach of Katsenelenbaum [23,24] and Wait [41]. According to that approach one should expand all fields over cylinder harmonics. For longitudinal components we have the following expressions:

$$\begin{aligned}
E_z^{sc} &= \sum_m \int dh e^{im\varphi+ihz} E_{z,mh}^{sc}(\rho) = \sum_m \int dh e^{im\varphi+ihz} H_m^{(1)}(\nu_2\rho) a_{mh} \\
E_z^{in} &= \sum_m \int dh e^{im\varphi+ihz} E_{0z,mh}(\rho) \\
E_z^{tr} &= \sum_m \int dh e^{im\varphi+ihz} J_m(\nu_1\rho) c_{mh} \\
B_z^{sc} &= \sum_m \int dh e^{im\varphi+ihz} H_m^{(1)}(\nu_2\rho) b_{mh} \\
B_z^{in} &= \sum_m \int dh e^{im\varphi+ihz} B_{0z,mh}(\rho) \\
B_z^{tr} &= \sum_m \int dh e^{im\varphi+ihz} J_m(\nu_1\rho) d_{mh}
\end{aligned} \tag{25}$$

Here superscripts *in*, *sc* and *tr* correspond to dipole field in free space, scattered and transmitted inside cylinder fields, respectively and $\nu_1 = \sqrt{\varepsilon k^2 - h^2}$ and $\nu_2 = \sqrt{k^2 - h^2}$ are radial wavenumbers. The a, b, c, d coefficients are to be determined. We choose the branch cut such as $Im(\nu_1), Im(\nu_2) > 0$ in complex plane of longitudinal wavenumber h . To ensure the decreasing of fields at space infinity ($\rho \rightarrow \infty$) the integration in (25) should be over path C_1 , which is shown in Fig.2.

The rest of the field components (ρ, φ) can be expressed through z-components of electric and magnetic fields:

$$\begin{aligned}
E_{\rho,mh} &= \frac{ih}{\nu^2} \frac{\partial E_{z,mh}}{\partial \rho} - \frac{km}{\rho\nu^2} B_{z,mh}; \\
E_{\varphi,mh} &= -\frac{hm}{\rho\nu^2} E_{z,mh} - \frac{ik}{\nu^2} \frac{\partial B_{z,mh}}{\partial \rho} \\
B_{\rho,mh} &= \frac{k\varepsilon m}{\rho\nu^2} E_{z,mh} + \frac{ih}{\nu^2} \frac{\partial B_{z,mh}}{\partial \rho} \\
B_{\varphi,mh} &= \frac{ik\varepsilon}{\nu^2} \frac{\partial E_{z,mh}}{\partial \rho} - \frac{mh}{\rho\nu^2} B_{z,mh};
\end{aligned} \tag{26}$$

In (25),(26) the subscripts m and h denote the appropriate Fourier transformation over φ and z , and $\nu = \nu_1$ or ν_2 for corresponding space region.

For free field one can obtain the following expressions [42]:

$$\begin{aligned}
\mathbf{B} &= rot\mathbf{A}, \quad \mathbf{E} = \frac{i}{k} rot\mathbf{H} \\
\mathbf{A} &= -ik\mathbf{d}_0 \frac{e^{ik|\mathbf{r}-\mathbf{r}'|}}{|\mathbf{r}-\mathbf{r}'|}
\end{aligned} \tag{27}$$

where $\mathbf{r} = (\rho, \varphi, z)$ and $\mathbf{r}' = (\rho', \varphi', z')$ are radius vectors of observation point and atom position.

Using well known expression [43]

$$\frac{e^{ik|\mathbf{r}-\mathbf{r}'|}}{|\mathbf{r}-\mathbf{r}'|} = \frac{i}{2} \sum_m \oint_{C_1} dh e^{im(\varphi-\varphi') + ih(z-z')} J_m(\nu_2 \rho_{<}) H_m^{(1)}(\nu_2 \rho_{>}) \quad (28)$$

where integration part should be as shown in Fig.2, one can find the expressions for longitudinal components of the fields on the fiber surface. For ρ oriented dipole in the region between fiber and dipole ($a \leq \rho < \rho'$) we have

$$\begin{aligned} B_{0z,mh} &= -\frac{id_{0,\rho} km}{2\rho'} J_m(\nu_2 \rho) H_m^{(1)}(\nu_2 \rho') \\ E_{0z,mh} &= \frac{d_{0,\rho} h \nu_2}{2} J_m(\nu_2 \rho) \frac{d}{dz} H_m^{(1)}(z) \Big|_{z=\nu_2 \rho'} \\ E_{0\varphi,mh} &= -\frac{md_{0,\rho}}{2\nu_2 \rho'} \left(k^2 \frac{d}{dz} J_m(z) \Big|_{z=\nu_2 \rho} H_m^{(1)}(\nu_2 \rho') + h^2 \frac{\rho'}{\rho} J_m(\nu_2 \rho) \frac{d}{dz} H_m^{(1)}(z) \Big|_{z=\nu_2 \rho'} \right) \\ B_{0\varphi,mh} &= \frac{ihkd_{0,\rho}}{2} \left(\frac{m^2}{\nu_2^2 \rho' \rho} J_m(\nu_2 \rho) H_m^{(1)}(\nu_2 \rho') + \frac{d}{dz} J_m(z) \Big|_{z=\nu_2 \rho} \frac{d}{dz} H_m^{(1)}(z) \Big|_{z=\nu_2 \rho'} \right) \end{aligned} \quad (29)$$

while for z oriented dipole we have

$$\begin{aligned} B_{0z,mh} &= 0 \\ E_{0z,mh} &= \frac{id_{0,z} \nu_2^2}{2} J_m(\nu_2 \rho) H_m^{(1)}(\nu_2 \rho') \\ E_{0\varphi,mh} &= -\frac{imhd_{0,z}}{2\rho} J_m(\nu_2 \rho) H_m^{(1)}(\nu_2 \rho') \\ B_{0\varphi,mh} &= -\frac{d_{0,z} k \nu_2}{2} \frac{d}{dz} J_m(z) \Big|_{z=\nu_2 \rho} H_m^{(1)}(\nu_2 \rho') \end{aligned} \quad (30)$$

Finally, for φ orientation of dipole momentum we have the following expressions

$$\begin{aligned} B_{0z,mh} &= -\frac{d_{0,\varphi} k \nu_2}{2} J_m(\nu_2 \rho) \frac{d}{dz} H_m^{(1)}(z) \Big|_{z=\nu_2 \rho'} \\ B_{0\varphi,mh} &= \frac{hkm d_{0,\varphi}}{2\nu_2 \rho} \left(J_m(\nu_2 \rho) \frac{d}{dz} H_m^{(1)}(z) \Big|_{z=\nu_2 \rho'} + \frac{\rho}{\rho'} H_m^{(1)}(\nu_2 \rho') \frac{d}{dz} J_m(z) \Big|_{z=\nu_2 \rho} \right) \\ E_{0z,mh} &= -\frac{id_{0,\varphi} hm}{2\rho'} J_m(\nu_2 \rho) H_m^{(1)}(\nu_2 \rho') \\ E_{0\varphi,mh} &= \frac{id_{0,\varphi}}{2} \left(k^2 \frac{d}{dz} J_m(z) \Big|_{z=\nu_2 \rho} \frac{d}{dz} H_m^{(1)}(z) \Big|_{z=\nu_2 \rho'} + \frac{h^2 m^2}{(\nu_2 \rho')(\nu_2 \rho)} J_m(\nu_2 \rho) H_m^{(1)}(\nu_2 \rho') \right) \end{aligned} \quad (31)$$

To find coefficients in transmitted and scattered fields one should take into account boundary conditions on the surface of dielectric cylinder. As a result we have a system of 4 equations for 4 unknown coefficients.

$$H_m^{(1)}(z_2) a_{mh} - J_m(z_1) c_{mh} = -e_{z,mh}(\rho = a)$$

$$H_m^{(1)}(z_2) b_{mh} - J_m(z_1) d_{mh} = -h_{z,mh}(\rho = a)$$

$$\frac{mh}{\nu_2^2 a} H_m^{(1)}(z_2) a_{mh} + \frac{ik}{\nu_2} \frac{d}{dz_2} H_m^{(1)}(z_2) b_{mh} - \frac{mh}{\nu_1^2 a} J_m(z_1) c_{mh} - \frac{ik}{\nu_1} \frac{d}{dz_1} J_m(z_1) d_{mh} = e_{\varphi,mh}(\rho = a)$$

$$\frac{ik}{\nu_2} \frac{d}{dz_2} H_m^{(1)}(z_2) a_{mh} - \frac{mh}{\nu_2^2 a} H_m^{(1)}(z_2) b_{mh} - \frac{ik\varepsilon}{\nu_1} \frac{d}{dz_1} J_m(z_1) c_{mh} + \frac{mh}{\nu_1^2 a} J_m(z_1) d_{mh} = -h_{\varphi,mh}(\rho = a) \quad (32)$$

where we use abbreviation $z_{1,2} = \nu_{1,2}a$.

The reflected electric fields are determined only by a_{mh} and b_{mh} coefficients, which can be simplified to

$$a_{mh} = \frac{na}{P^2 + QR}, \quad b_{mh} = \frac{nb}{P^2 + QR} \quad (33)$$

where

$$na = \nu_1^2 \nu_2^2 a J_m(z_1) P E_{0\varphi,mh} + \nu_2^2 \left(J_m(z_1) h m P + k a \varepsilon \nu_1 \frac{d}{dz_1} J_m(z_1) Q \right) E_{0z,mh} \quad (34)$$

$$+ i \nu_1^2 \nu_2^2 a J_m(z_1) Q B_{0\varphi,mh} - i m h \nu_1 \nu_2 J_m(z_1) S B_{0z,mh}$$

$$nb = \nu_1^2 \nu_2^2 a J_m(z_1) P B_{0\varphi,mh} + \nu_2^2 \left(J_m(z_1) h m P - a k \nu_1 \frac{d}{dz_1} J_m(z_1) R \right) B_{0z,mh} \quad (35)$$

$$+ i \nu_1^2 \nu_2^2 a J_m(z_1) R E_{0\varphi,mh} + i m h \nu_1 \nu_2 J_m(z_1) T E_{0z,mh}$$

and

$$P = h m k^2 J_m(z_1) H_m^{(1)}(z_2) (\varepsilon - 1)$$

$$Q = -\nu_1 \nu_2 a k \left(\nu_1 J_m(z_1) \frac{d}{dz_2} H_m^{(1)}(z_2) - \nu_2 H_m^{(1)}(z_2) \frac{d}{dz_1} J_m(z_1) \right)$$

$$R = \nu_1 \nu_2 a k \left(\nu_1 J_m(z_1) \frac{d}{dz_2} H_m^{(1)}(z_2) - \nu_2 \varepsilon H_m^{(1)}(z_2) \frac{d}{dz_1} J_m(z_1) \right) \quad (36)$$

$$S = \nu_1 \nu_2 a k \left(\nu_2 J_m(z_1) \frac{d}{dz_2} H_m^{(1)}(z_2) - \nu_1 H_m^{(1)}(z_2) \frac{d}{dz_1} J_m(z_1) \right)$$

$$T = \nu_1 \nu_2 a k \left(\nu_2 J_m(z_1) \frac{d}{dz_2} H_m^{(1)}(z_2) - \nu_1 \varepsilon H_m^{(1)}(z_2) \frac{d}{dz_1} J_m(z_1) \right)$$

Finally for decay rates we have the following expressions

$$\left(\frac{\gamma}{\gamma_0} \right)_\rho = 1 + \frac{3}{2} I m \frac{\sum_m \oint_{C_1} dh \frac{1}{\nu_2^2} \left[i h \nu_2 \frac{d}{dz} H_m^{(1)}(z) a_{mh} - \frac{k m}{\rho'} H_m^{(1)}(z) b_{mh} \right]_{z=\nu_2 \rho'}}{d_{0,\rho} k^3} \quad (37)$$

$$\left(\frac{\gamma}{\gamma_0} \right)_\varphi = 1 + \frac{3}{2} I m \frac{\sum_m \oint_{C_1} dh \frac{1}{\nu_2^2} \left[-i k \nu_2 \frac{d}{dz} H_m^{(1)}(z) b_{mh} - \frac{h m}{\rho'} H_m^{(1)}(z) a_{mh} \right]_{z=\nu_2 \rho'}}{d_{0,\varphi} k^3} \quad (38)$$

$$\left(\frac{\gamma}{\gamma_0}\right)_z = 1 + \frac{3}{2}Im \frac{\sum_m \oint_{C_1} dh H_m^{(1)}(\nu_2 \rho') a_{mh}}{d_{0,z} k^3} \quad (39)$$

As it was mentioned above, the important feature of dielectric fiber is the presence of guided modes, which differs substantially from free space spherical waves. Such modes are effectively used in optical communications lines. Note there are no such modes in the case of dielectric sphere or ideally conducting cylinder. So-called whispering gallery modes are decaying ones even in the case of lossless materials.

Thus there are two types of modes in presence of dielectric fiber: free space radiation modes and wave guiding modes. From mathematical point of view these modes correspond to different types of spectrum. The guided modes correspond to discrete spectrum while radiating modes correspond to continuous part of spectrum. In this connection the expressions (37)-(39) are not fully suitable for further analysis, because the guided modes are not separated here.

The appearance of guided modes is connected with poles in subintegral expressions (37),(38) and (39). One can show that in the case of lossless dielectric these poles are situated on the real axis of h between k and $k\sqrt{\varepsilon}$ and the number of poles is finite [23,24].

Now transforming integration contour from C_1 to C_2 as it is shown in Fig.2 and applying the residue theorem, it is possible to separate radiating and guided modes

$$\begin{aligned} \left(\frac{\gamma}{\gamma_0}\right)_\rho = 1 + \frac{3}{2}Im \frac{\sum_m \oint_{C_2} dh \frac{1}{\nu_2} \left[ih\nu_2 \frac{d}{dz} H_m^{(1)}(z) a_{mh} - \frac{km}{\rho'} H_m^{(1)}(z) b_{mh} \right]_{z=\nu_2 \rho'}}{d_{0,\rho} k^3} \\ + 3\pi Re \sum_m \sum_{h_\alpha} Res \left[\frac{\frac{1}{\nu_2} \left[ih\nu_2 \frac{d}{dz} H_m^{(1)}(z) a_{mh} - \frac{km}{\rho'} H_m^{(1)}(z) b_{mh} \right]_{z=\nu_2 \rho'}}{d_{0,\rho} k^3} \right]_{h=h_{a,m}} \end{aligned} \quad (40)$$

$$\begin{aligned} \left(\frac{\gamma}{\gamma_0}\right)_\varphi = 1 + \frac{3}{2}Im \frac{\sum_m \oint_{C_2} dh \frac{1}{\nu_2} \left[-ik\nu_2 \frac{d}{dz} H_m^{(1)}(z) b_{mh} - \frac{hm}{\rho'} H_m^{(1)}(z) a_{mh} \right]_{z=\nu_2 \rho'}}{d_{0,\varphi} k^3} \\ + 3\pi Re \sum_m \sum_{h_\alpha} Res \left[\frac{\frac{1}{\nu_2} \left[-ik\nu_2 \frac{d}{dz} H_m^{(1)}(z) b_{mh} - \frac{hm}{\rho'} H_m^{(1)}(z) a_{mh} \right]_{z=\nu_2 \rho'}}{d_{0,\varphi} k^3} \right]_{h=h_{a,m}} \end{aligned} \quad (41)$$

$$\begin{aligned} \left(\frac{\gamma}{\gamma_0}\right)_z = 1 + \frac{3}{2}Im \frac{\sum_m \oint_{C_2} dh \left[H_m^{(1)}(z) a_{mh} \right]_{z=\nu_2 \rho'}}{d_{0,z} k^3} \\ + 3\pi Re \sum_m \sum_{h_{\alpha,m}} Res \left[\frac{\left[H_m^{(1)}(z) a_{mh} \right]_{z=\nu_2 \rho_0}}{d_{0,z} k^3} \right]_{h=h_{a,m}} \end{aligned} \quad (42)$$

where the sum is over all poles $h_{\alpha,m}$ of subintegral functions and *Res* means residue.

In expressions (40)-(42) the first term corresponds to spherical waves running to infinity, while the second term corresponds to guided modes. It should be emphasized that in the

case of lossless media the vertical part of branch cut (along imaginary axis of h) gives no contribution to decay rates. From physical point of view it is due to the exponential decrease of corresponding spherical waves when moving away from cylinder. For lossy media this branch is very important because it describes nonradiative losses. The nonradiative decay rates found in previous section (expressions (23)) is the asymptote of integral over the vertical part of branch cut when ka moves to zero.

As it was mentioned above, in the dielectric case there is only finite number of guided modes with longitudinal wavevectors between k and $k\sqrt{\varepsilon}$. Moreover, for small enough fiber (for nanofiber!) with

$$ka < \frac{2.4}{\sqrt{\varepsilon - 1}} \quad (43)$$

the only one guided mode with $m = \pm 1$ exists. Sometimes such modes are referred to as main or principal modes.

The dependence of longitudinal wavenumber h on cylinder radius or frequency is determined by dispersion equation

$$D = P^2 + QR = 0, \quad m = \pm 1 \quad (44)$$

where P , Q and R are defined by (36).

In the case of nanofibers, $ka \ll 1$, the asymptotic solution of (44) can be presented in the form:

$$\frac{h}{k} = 1 + \frac{2}{(ka)^2} \exp \left(-\frac{2}{(ka)^2} \frac{\varepsilon + 1}{\varepsilon - 1} + \frac{\varepsilon + 1}{4} - 2\gamma + \dots \right) \quad (45)$$

where $\gamma = 0.5776$ - Euler constant.

The exact and asymptotic solution of (44) are shown in Fig.3, where one can see that asymptote (45) present solution of (44) correctly if $ka < 0.8$. In what follows we restrict ourselves to the case of nanofiber, when condition (43) holds true.

To calculate decay rates into guided modes one should know the residues of corresponding expression. These residues can be found if one know the asymptotic behavior of resonant denominator near pole. In the case of nanofiber the denominator can be approximated by

$$D = P^2 + QR \approx k^6 \frac{(\varepsilon - 1)^3}{\pi^2} (ka)^2 \left((h/k) / (h/k)_{10} - 1 \right) \quad (46)$$

where $\left(\frac{h}{k} \right)_{10}$ is given by (45).

Let us stress once more that the expressions (42) - (42), (45), (46) are valid in the case of complex dielectric permittivity. In the case of metallic cylinder, that is in the case when $\text{Re}(\varepsilon) < 0$, the poles of subintegral function are also near the real axis of h . But now they corresponds to plasmon resonances. More detailed investigation of plasmon resonance influence on decay rate will be presented in separate publication [35].

IV. DECAY RATES NEAR SURFACE OF NANOFIBER WITHOUT LOSSES.

The expressions (42) - (42) fully describe the problem of spontaneous emission of an atom placed near cylinder made of any material. However, these expressions are too complicated to understand real picture of decay rate. Our goal is to find simple analytical expressions allowing to estimate decay rate near cylinder with radius, which is substantially small in comparison with wavelength, $ka \ll 1$. Moreover to obtained simple asymptotes we restricts ourselves to the case of an atom placed on the surface ($\rho' \rightarrow a$) of lossless dielectric cylinder.

A. z-orientation of dipole

Substituting the expression for exciting external fields (30) into general expression for decay rate (42) one can represent the decay rate for z-oriented dipole momentum in the form:

$$\begin{aligned} \left(\frac{\gamma}{\gamma_0}\right)_z &= 1 - \frac{3}{2} Re \sum_m \int_0^k \frac{d\nu \nu_2^2}{k^3} \frac{H_m^{(1)}(\nu_2 \rho')^2 J_m(z_2)}{H_m^{(1)}(z_2)} \\ &- \frac{3}{\pi} Im \sum_m \int_0^k \frac{d\nu \nu_1^2 \nu_2^2}{k^2} \frac{H_m^{(1)}(\nu_2 \rho')^2 J_m(z_1) Q}{H_m^{(1)}(z_2) D} \\ &- 3 Re \sum_m \sum_{h_{\alpha, m}} \text{Res} \left[\frac{\nu_1^2 \nu_2^2}{k^2} \frac{H_m^{(1)}(\nu_2 \rho')^2 J_m(z_1) Q}{H_m^{(1)}(z_2) D} \right]_{h_{\alpha, m}} \end{aligned} \quad (47)$$

where Q and D are defined by (36) and (44), and $z_{1,2} = \nu_{1,2} a$.

Note, the first line of (47) coincides with decay rate near ideally conducting cylinder [22]. This expression is valid for real dielectric permittivities.

In the most interesting case of an atom near surface of nanofiber ($\rho' = a$) using identity $\sum_m J_m^2(z) = 1$ one can simplify (47) to more compact form

$$\begin{aligned} \left(\frac{\gamma}{\gamma_0}\right)_z &= -\frac{3}{\pi} Im \sum_m \int_0^k \frac{d\nu \nu_1^2 \nu_2^2}{k^2} \frac{H_m^{(1)}(z_2) J_m(z_1) Q}{D} \\ &- 3 Re \sum_m \sum_{h_{\alpha}} \left[\frac{\nu_1^2 \nu_2^2}{k^2} \frac{H_m^{(1)}(z_2) J_m(z_1) Q}{D} \right]_{h_{\alpha, m}} \end{aligned} \quad (48)$$

The asymptote of (48) for $ka \ll 1$ has the following form

$$\begin{aligned} \left(\frac{\gamma}{\gamma_0}\right)_z &\approx 1 - \frac{(\varepsilon-1)}{75} \left(60(\gamma + \ln ka) - 47 - \frac{45\varepsilon-15}{(\varepsilon+1)^2} \right) (ka)^2 + O((ka)^4) \\ &+ \frac{12}{(ka)^4} \exp \left(-\frac{2}{(ka)^2} \frac{\varepsilon+1}{\varepsilon-1} + \frac{\varepsilon+1}{4} - 2\gamma \right) \end{aligned} \quad (49)$$

Here the first line describes the radiative losses while exponentially small second line describes contribution of the main guided mode.

B. φ oriented dipole

Let us now consider the case of dipole with φ orientation of dipole momentum and located in close vicinity to the surface of nanofiber ($\rho' \rightarrow a$). In the case of lossless media the general expression (41) can be simplified to

$$\begin{aligned} \left(\frac{\gamma}{\gamma_0}\right)_\varphi &= 1 - \frac{3}{2} Re \sum_{m=-\infty}^{\infty} \int_0^k \frac{dh}{k} \left[\frac{h^2 m^2}{k^2 z_2^2} J(z_2) H(z_2) + H'(z_2) J'(z_2) \right] - \\ &+ \frac{3}{\pi} Im \sum_{m=-\infty}^{\infty} \int_0^k dh \frac{h^2 m^2 \nu_2 J(z_1) H(z_2) (\nu_2^3 J(z_1) H'(z_2) - \nu_1^3 J'(z_1) H(z_2)) + \nu_1 \nu_2^2 ka H'(z_2) J'(z_1) R}{k z_2 D} \\ &+ 3 Re \sum_{m=-\infty}^{\infty} \sum_{h_{\alpha,m}} \text{Res} \left[\frac{h^2 m^2 \nu_2 J(z_1) H(z_2) (\nu_2^3 J(z_1) H'(z_2) - \nu_1^3 J'(z_1) H(z_2)) + \nu_1 \nu_2^2 ka H'(z_2) J'(z_1) R}{k z_2 D} \right]_{h_{\alpha,m}} \end{aligned} \quad (50)$$

where D is defined by (44). Here for brevity we omit indices (m) in Bessel and Hankel functions of first kind and use prime to denote derivative of Hankel and Bessel functions.

Using the identities

$$\sum_{n=-\infty}^{n=\infty} J_n^2(z) = 1; \quad \sum_{n=-\infty}^{n=\infty} n^2 J_n^2(z) = \frac{z^2}{2}; \quad \sum_{n=-\infty}^{n=\infty} \left(\frac{dJ_n(z)}{dz} \right)^2 = \frac{1}{2} \quad (51)$$

one can show that first line in (50) is equal to zero. Finally the expression for radiative decay rate of an φ -oriented dipole placed on the surface of nanofiber acquires the following form

$$\begin{aligned} \left(\frac{\gamma}{\gamma_0}\right)_\varphi &= \frac{3}{\pi} Im \sum_{m=-\infty}^{\infty} \int_0^k dh \frac{h^2 m^2 \nu_2 J(z_1) H(z_2) (\nu_2^3 J(z_1) H'(z_2) - \nu_1^3 J'(z_1) H(z_2)) + \nu_1 \nu_2^2 ka H'(z_2) J'(z_1) R}{k z_2 D} \\ &+ 3 Re \sum_{m=-\infty}^{\infty} \sum_{h_{\alpha,m}} \text{Res} \left[\frac{h^2 m^2 \nu_2 J(z_1) H(z_2) (\nu_2^3 J(z_1) H'(z_2) - \nu_1^3 J'(z_1) H(z_2)) + \nu_1 \nu_2^2 ka H'(z_2) J'(z_1) R}{k z_2 D} \right]_{h_{\alpha,m}} \end{aligned} \quad (52)$$

The asymptote of (52) for $ka \ll 1$ has the following form

$$\begin{aligned} \left(\frac{\gamma}{\gamma_0}\right)_\varphi &= \left(\frac{2}{\varepsilon+1}\right)^2 + \frac{(\varepsilon-1)(75\varepsilon^2+2081-1680(\gamma+\ln(ka)))(ka)^2}{300(\varepsilon+1)^3} + O((ka)^4) \\ &+ \frac{48}{(\varepsilon-1)^2(ka)^6} \exp\left(-\frac{2}{(ka)^2} \frac{\varepsilon+1}{\varepsilon-1} + \frac{\varepsilon+1}{4} - 2\gamma\right) \end{aligned} \quad (53)$$

Here the first line describes the radiative losses while exponentially small second line describes contribution of the main guided mode.

C. ρ - oriented dipole

The case of radially oriented dipole momentum is more complicated for analysis. So we again restrict ourselves to the most interesting case, when atom is near dielectric surface,

that is we consider $\rho' = a$ case. In the case of lossless media the general expression (40) can be simplified to

$$\begin{aligned} \left(\frac{\gamma}{\gamma_0}\right)_\rho &= 1 - \frac{3}{2}Re \sum_{m=-\infty}^{\infty} \int_0^k \frac{dh}{k} \frac{h^2}{k^2} H'^2(z_2) \frac{J(z_2)}{H(z_2)} + \frac{m^2 H(z_2) J(z_2)}{z_2^2} - \\ &- \frac{2iv_1^2}{\pi k z_2^2} \frac{J(z_1)}{H(z_2)} \left\{ \frac{2h^2 k^3 m^2 z_2 (\varepsilon - 1) J(z_1) H(z_2)^2 H'(z_2) + z_2^2 h^2 Q H'^2(z_2) - m^2 k^2 H(z_2)^2 R}{D} \right\} \\ &- 3Re \sum_{m=-\infty}^{\infty} \sum_{h_{\alpha,m}} \left[\frac{v_1^2}{k^2 z_2^2} \frac{J(z_1)}{H(z_2)} \left\{ \frac{2h^2 k^3 m^2 z_2 (\varepsilon - 1) J(z_1) H(z_2)^2 H'(z_2) + z_2^2 h^2 Q H'^2(z_2) - m^2 k^2 H(z_2)^2 R}{D} \right\} \right]_{h_{\alpha,m}} \end{aligned} \quad (54)$$

where D is defined by (44).

In the case $\varepsilon \rightarrow \infty$, from integral over cut (first two lines in (54)) one can reveal the decay rate for an atom near ideally conducting cylinder [22].

$$\left(\frac{\gamma}{\gamma_0}\right)_\rho = \frac{6}{\pi^2} \sum_{n=-\infty}^{\infty} \int_0^k dh \frac{h^2}{k^3 (\nu a)^2} \frac{1}{|H_n^{(1)}(\nu a)|^2} + \frac{6}{\pi^2} \sum_{n=-\infty}^{\infty} \int_0^k dh \frac{n^2}{k (\nu a)^4} \frac{1}{\left| \frac{d}{dz} \left(H_n^{(1)}(z) \right) \right|_{z=\nu a}^2} \quad (55)$$

what confirms rather complicated algebra.

The analysis shows that for the case of cylinder of small radius $ka\sqrt{\varepsilon - 1} < j_{0,1} \approx 2.4048$ only residue from term with $m=1$ will give contribution. As a result, the asymptote of decay rate of atom placed on the surface of small dielectric fiber takes the following form $ka \rightarrow 0$:

$$\begin{aligned} \left(\frac{\gamma}{\gamma_0}\right)_\rho &= \left(\frac{2\varepsilon}{\varepsilon+1}\right)^2 + \frac{\varepsilon^2(\varepsilon-1)(15\varepsilon^2+60\varepsilon+2201-1680(\gamma+\ln(ka)))(ka)^2}{300(\varepsilon+1)^3} + O((ka)^4) \\ &+ \frac{48\varepsilon^2}{(\varepsilon-1)^2(ka)^6} \exp\left(-\frac{2}{(ka)^2} \frac{\varepsilon+1}{\varepsilon-1} + \frac{\varepsilon+1}{4} - 2\gamma\right) \end{aligned} \quad (56)$$

Here the first line describes the radiative losses while exponentially small second line describes contribution of the main guided mode.

V. GRAPHICS ILLUSTRATIONS AND DISCUSSIONS

We should note before all that asymptotes (49), (53) and (56) do agree with quasistatic results (17) in the limit $ka \rightarrow 0$. It proves quasistatic calculations and confirms complicated algebra of full electrodynamics case.

Another interesting case is the case of large dielectric permittivity. This case should be treated carefully because the limits $ka \rightarrow 0$ and $\varepsilon \rightarrow \infty$ do not commute. That is why one can not use our asymptotes for large enough ε . To investigate the case of $\varepsilon \rightarrow \infty$, one should take limit of general expressions (48), and only then investigate asymptotes for $ka \rightarrow 0$. The analogous situation takes place in the case of planar interface [44] or for atom near prolate nanospheroid [33,34].

Now, combining results from sections 2 and 4 we can write the total decay rate of an atom near nanofiber with small losses in the following form

$$\left(\frac{\gamma}{\gamma_0}\right)^{total} = \left(\frac{\gamma}{\gamma_0}\right)^{nonradiative} + \left(\frac{\gamma}{\gamma_0}\right)^{guided} + \left(\frac{\gamma}{\gamma_0}\right)^{radiative} \quad (57)$$

where

$$\left(\frac{\gamma}{\gamma_0}\right)_\rho^{nonradiative} = -\frac{3}{\pi k^3} \sum_{m=0}^{\infty} (2 - \delta_{m,0}) \int_0^{\infty} dh h^2 K_m'^2(h\rho') \operatorname{Im}(G_m(ha))$$

$$\left(\frac{\gamma}{\gamma_0}\right)_\varphi^{nonradiative} = -\frac{6}{\pi k^3} \sum_{m=0}^{\infty} \frac{m^2}{\rho'^2} \int_0^{\infty} dh K_m^2(h\rho') \operatorname{Im}(G_m(ha))$$

$$\left(\frac{\gamma}{\gamma_0}\right)_z^{nonradiative} = -\frac{3}{\pi k^3} \sum_{m=0}^{\infty} (2 - \delta_{m,0}) \int_0^{\infty} dh h^2 K_m^2(h\rho') \operatorname{Im}(G_m(ha))$$

$$\left(\frac{\gamma}{\gamma_0}\right)_\rho^{guided} = \frac{48\varepsilon^2}{(\varepsilon - 1)^2 (ka)^6} \exp\left(-\frac{2}{(ka)^2} \frac{\varepsilon + 1}{\varepsilon - 1} + \frac{\varepsilon + 1}{4} - 2\gamma\right)$$

$$\left(\frac{\gamma}{\gamma_0}\right)_\varphi^{guided} = \frac{48}{(\varepsilon - 1)^2 (ka)^6} \exp\left(-\frac{2}{(ka)^2} \frac{\varepsilon + 1}{\varepsilon - 1} + \frac{\varepsilon + 1}{4} - 2\gamma\right)$$

$$\left(\frac{\gamma}{\gamma_0}\right)_z^{guided} = \frac{12}{(ka)^4} \exp\left(-\frac{2}{(ka)^2} \frac{\varepsilon + 1}{\varepsilon - 1} + \frac{\varepsilon + 1}{4} - 2\gamma\right)$$

$$\left(\frac{\gamma}{\gamma_0}\right)_\rho^{radiative} = \left|1 + \frac{\varepsilon - 1}{\varepsilon + 1} \frac{a^2}{\rho'^2}\right|^2 + \frac{\varepsilon^2 (\varepsilon - 1) (15\varepsilon^2 + 60\varepsilon + 2201 - 1680(\gamma + \ln(ka))) (ka)^2}{300 (\varepsilon + 1)^3}$$

$$\left(\frac{\gamma}{\gamma_0}\right)_\varphi^{radiative} = \left|1 - \frac{\varepsilon - 1}{\varepsilon + 1} \frac{a^2}{\rho'^2}\right|^2 + \frac{(\varepsilon - 1) (75\varepsilon^2 + 2081 - 1680(\gamma + \ln(ka))) (ka)^2}{300 (\varepsilon + 1)^3}$$

$$\left(\frac{\gamma}{\gamma_0}\right)_z^{radiative} = 1 - \frac{(\varepsilon - 1)}{75} \left(60(\gamma + \ln ka) - 47 - \frac{45\varepsilon - 15}{(\varepsilon + 1)^2}\right) (ka)^2$$

These expressions are the main result of the work and allow to estimate decay rates of an atom placed near nanofiber with $ka \ll 1$.

However, it is difficult to say when these results are valid in practice. To find region of applicability of our results we calculated the decay rates according to full formulae and compare them with asymptotes (57). The results of comparison are presented in Fig. 4-12.

First of all from the Fig. 4,7,10 one can see that our asymptotic expansions are good enough for $ka < 0.4(\varepsilon = 3)$. When the dielectric permittivity is increased the region of applicability of longwave asymptotes reduces. For $\varepsilon = 10$ (Fig. 5,8,11) applicability region is $ka < 0.1$, while for $\varepsilon = 30$ (Fig. 6,9,12) applicability region is $ka < 0.05$. One can suppose that generally our results are valid for

$$ka < 1/\varepsilon. \quad (58)$$

This region corresponds to very thin nanofiber. For example, for $\varepsilon=3$ fiber radius should be about $\lambda/20$!

The rest of nanofiber radii,

$$1/\varepsilon < ka < 2.4/\sqrt{\varepsilon - 1} \quad (59)$$

should be analyzed numerically (see Fig.4-12). From these figures one can see that for large enough nanofibers (59), the decay rates increase with increasing of dielectric permittivity. The most substantial enhancement is observed for ρ and z orientations, where enhancement of total decay rates can reach value about 35 and 23 for $\varepsilon=30$ (Fig.6,9). The most important feature of ρ and z orientations of dipole momentum is very efficient excitation of guided modes. On the contrary, the influence of guided modes on spontaneous emission of φ -oriented dipole is rather small.

To trace the influence of guided mode on total decay rate we plot the ratio of decay rate into guided modes to total decay rate

$$\beta = \frac{\left(\frac{\gamma}{\gamma_0}\right)^{guided}}{\left(\frac{\gamma}{\gamma_0}\right)^{guided} + \left(\frac{\gamma}{\gamma_0}\right)^{radiative}} \quad (60)$$

This quantity is very important for determining the laser threshold [45]. From Fig. 13-15 it is seen that the spontaneous emission coupling efficiency β is rather high for ρ and z orientations even in the case of monomode nanofibers! It is interesting that the asymptote describes the coupling efficiency well in rather wide region (Fig.13). The dipoles with φ orientations of momentum have the small spontaneous emission coupling efficiency (Fig.14)

Finally, In the Fig.16 the total decay rates near nanofiber are compared with decay rates near ideally conducting cylinder. From this figures one can see that for large enough dielectric permittivity the decay rate near nanofiber can be greater than decay rate near ideally conducting cylinder. Again these effect is due to excitation of principle mode in nanofiber.

VI. CONCLUSION

In the present paper the decay rates of an excited atom placed near a dielectric fiber is considered. The main attention was paid to the case of cylinder with radius which is small in comparison with radiation wavelength (nanofiber), $ka < 2.4/\sqrt{\varepsilon - 1}$. The decay rates are found within quasistatic as well as full electrodynamics approaches. It is proved that quasistatic approximation works well for nanofiber with $ka < 1/\varepsilon$. In contrast to quasistatic solution the exact one has additional terms from guided modes, which exists even for nanofiber of arbitrary small radius. However the contributions from such modes decreases exponentially when cylinder radius tends to zero. For large enough nanofiber, $1/\varepsilon < ka < 2.4/\sqrt{\varepsilon - 1}$, the influence of guided modes on the decay rate is substantial.

The results obtained can be useful as for estimation of decay rates and for understanding of interplay between different decay channels. The results obtained is in agreement with those for an atom placed near dielectric or metallic nanospheroid

In present paper we pay attention to the case of dielectric nanofiber with positive dielectric permittivity. However, our results can be applied to investigation of decay rates near metallic nanowire with negative dielectric constant. In the case of nanowires the quasistatic expressions (16) remain valid, but one should add to them contribution, which is due to excitation of plasmon resonances. The detailed analysis of decay rates of an atom placed near nanowires will be presented elsewhere [35].

Acknowledgements

The authors thank the Russian Basic Research Foundation (V.K.) , Center “Integration” and Centre National De La Recherche Scientifique for financial support of this work.

REFERENCES

- [1] E.M. Purcell , *Phys. Rev.* **69**, 681 (1946).
- [2] *Cavity Quantum Electrodynamics*, edited by P.Berman, (Academic, New York, 1994).
- [3] Zh.I. Alferov , Nobel Lecture (2000).
- [4] W.Lucosz, R.E.Kunz, *Opt.Comm.* **20**, 195 (1977).
- [5] G.Barton, *J. Phys.* **B16**, 2134 (1974).
- [6] M.Babiker, G.Barton, *J. Phys.* **A9**, 129 (1976).
- [7] G. Barton, Van der Waals shifts in an atom near absorptive dielectric mirrors, *Proc.R.Soc. Lond.* **A453**, 2461(1997).
- [8] M.Fichet, F.Schuller, D.Bloch, and M.Ducloy *Phys.Rev.* **A51**, 1533, (1995)
- [9] M.-P.Gorza, S.Saltiel, H.Failache and M.Ducloy. *The European Physical Journal* **D15**, 113(2001).
- [10] H.Nha, W.Jhe, Cavity quantum electrodynamics between parallel dielectric surfaces, *Phys.Rev.* **A 54**, 3505 (1996).
- [11] J. Denschlag, G. Umshaus , J. Schmiedmayer , *Phys. Rev. Lett*, **81**, 737(1998).
- [12] J. Denschlag, D.Cassetari , A. Chenet , S. Schneider , J. Schmiedmayer, *Appl. Phys.* **B69** , 291(1999) .
- [13] W.A. Lyon, S.M. Nie, *Anal. Chem.* **69**, 3400 (1997).
- [14] C. Zander, K.H. Drexhage, K.T. Han, J. Wolfrum, M. Sauer, *Chem. Phys. Lett.* **286**, 457 (1998).
- [15] D.Y. Chu, S.T. Ho, Spontaneous emission from excitons in cylindrical dielectric waveguides and the spontaneous emission factor of microcavity ring laser, *J. Optical Society of America* **B10**, 381 (1993).
- [16] D.Y. Chu, S.T. Ho, J.P.Zhang and M.K.Chin, Dielectric Photonic Wells and Wires and Spontaneous Emission Coupling Efficiency of Microdisk and Photonic-Wire Semiconductor Lasers, In: *Optical Processes in Microcavities*, R.K. Chang, A.J. Campillo (eds.), Word Scientific, 1996, P.339-389
- [17] C. Dekker, Carbon Nanotubes as Molecular Quantum wires.- *Physics Today*, May, P.22 (1999).
- [18] R. Saito, G. Dresselhaus, M.S. Dresselhaus, *Physical Properties of Carbon Nanotubes*, Imperial College Press, London, 1998.
- [19] S.D.Brorson, H.Yokoyama, E.P.Ippen, Spontaneous Emission Rate Alteration in Optical Waveguide structures, *IEEE Journ. of Quant. Electronics* **26**, 1492 (1990).
- [20] S.D.Brorson, P.M.W.Skovgaard, Optical mode density and spontaneous emission in microcavities, In: *Optical Processes in Microcavities*, R.K. Chang, A.J.Campillo (eds.), Word Scientific, 1996, P.339-389
- [21] M.A. Rippin, P.L. Knight, Modified spontaneous emission in a cylindrical microcavities: guided and distributed Bragg reflecting structures, *Journ. Mod. Optics* **43**, 807 (1996).
- [22] V.V. Klimov, M.Ducloy , Allowed and forbidden transitions in an atom placed near an ideally conducting cylinder - *Phys. Rev.* **A62**, 043818(2000).
- [23] B.Z. Katsenelenbaum , *Zhurnal Tekhnicheskoi fiziki* **XIX**, 1168(1949) (In Russian).
- [24] B.Z. Katsenelenbaum , *Zhurnal Tekhnicheskoi fiziki* **XIX**, 1182(1949) (In Russian).
- [25] H. Nha, W. Jhe, Cavity Quantum Electrodynamics for a cylinder: Inside a hollow dielectric and near a solid dielectric cylinder, *Phys.Rev.***A56**, 2213(1997).
- [26] J. Enderlein , *Chem. Phys.Lett.* **301**, 430 (1999).

- [27] W. Zakowicz, M. Janowicz, Phys. Rev. **A62**, 013820 (2000).
- [28] T. Søndergaard and B. Tromborg, General theory for spontaneous emission in active dielectric microstructures: Example of a fiber amplifier, Phys. Rev. **A64**, 033812 (2001).
- [29] S.A. Maksimenko, G.Ya. Slepian, Radiotekhnika i Elektronika, **47**, 261 (2002) (In Russian)
- [30] I.V. Bondarev, S.A. Maksimenko, G.Ya. Slepian, arXiv:cond-mat/0204433v12 19 April 2002
- [31] W.R. Smythe, *Static and Dynamic Electricity*, Third Edition, A SUMMA Book, 1989.
- [32] M. Abramowitz and I.A. Stegun, eds., *Handbook of Mathematical Functions* (M. NBS, 1964).
- [33] V.V. Klimov, M. Ducloy, and V.S. Letokhov, *Kvantovaya Elektronika*, **31**, 569 (2001).
- [34] V.V. Klimov, M. Ducloy, and V.S. Letokhov, Spontaneous emission of an atom placed near a prolate nanospheroid, European Physical Journal D, 2002 (in print).
- [35] V.V. Klimov, M. Ducloy, Spontaneous emission of single atom placed near metallic nanowires (to be published)
- [36] R.R. Chance, A. Prock, R. Sylbey, Adv. Chem. Phys. **37**, 1 (1978).
- [37] J.M. Wylie, J.E. Sipe, Phys. Rev. **A30**, 1185 (1984); **A32**, 2030 (1985).
- [38] L. Knöll, S. Scheel, and Dirk-Gunnar Welsch, *QED in Dispersing and Absorbing Dielectric Media*, Quant-ph/000621-27 June 2000
- [39] Ho Trung Dung, Ludwig Knöll, and Dirk-Gunnar Welsch, Phys. Rev. **A64**, 013804 (2001)
- [40] A.F. Stevenson, *J. Appl. Phys.*, **24**, 1134 (1953).
- [41] J.R. Wait, *Electromagnetic Radiation from Cylindrical Structures*, Pergamon Press, New York, 1959.
- [42] J.D. Jackson, *Classical electrodynamics*. (Wiley, New York, 1975).
- [43] G.T. Markov, A.F. Chaplin, *Excitation of electromagnetic waves*, Moscow, Radio I Svyaz, 1983, 296p. (In Russian).
- [44] Wu B.S.T., Eberlein C., Proc. R. Soc. Lond. **A455**, 2487 (1998).
- [45] Y. Yamamoto, *Coherence, amplification and quantum effects in semiconductor lasers*, (John Wiley & Sons, Inc., New York, 1991).

FIGURES

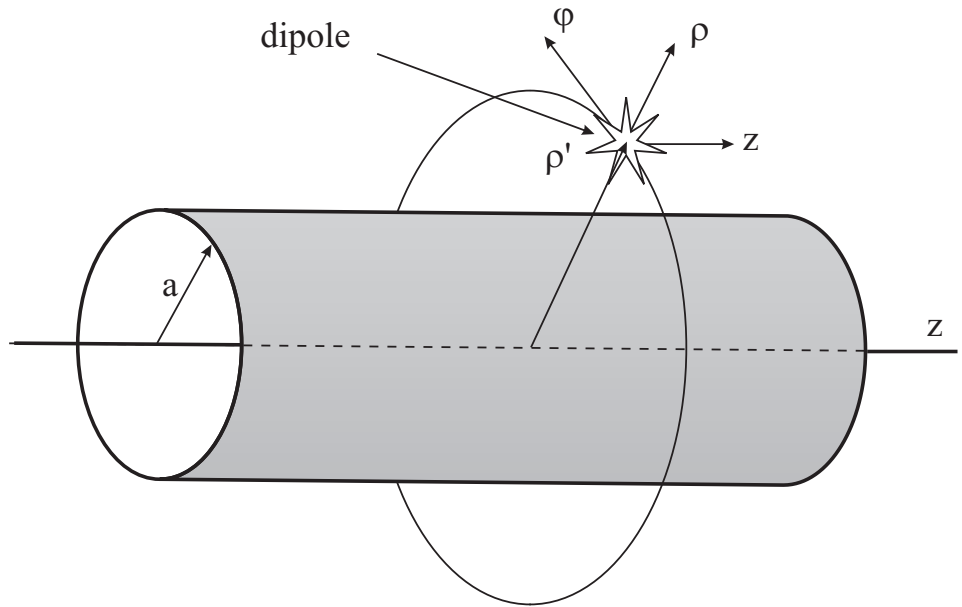


FIG. 1. Geometry of the problem

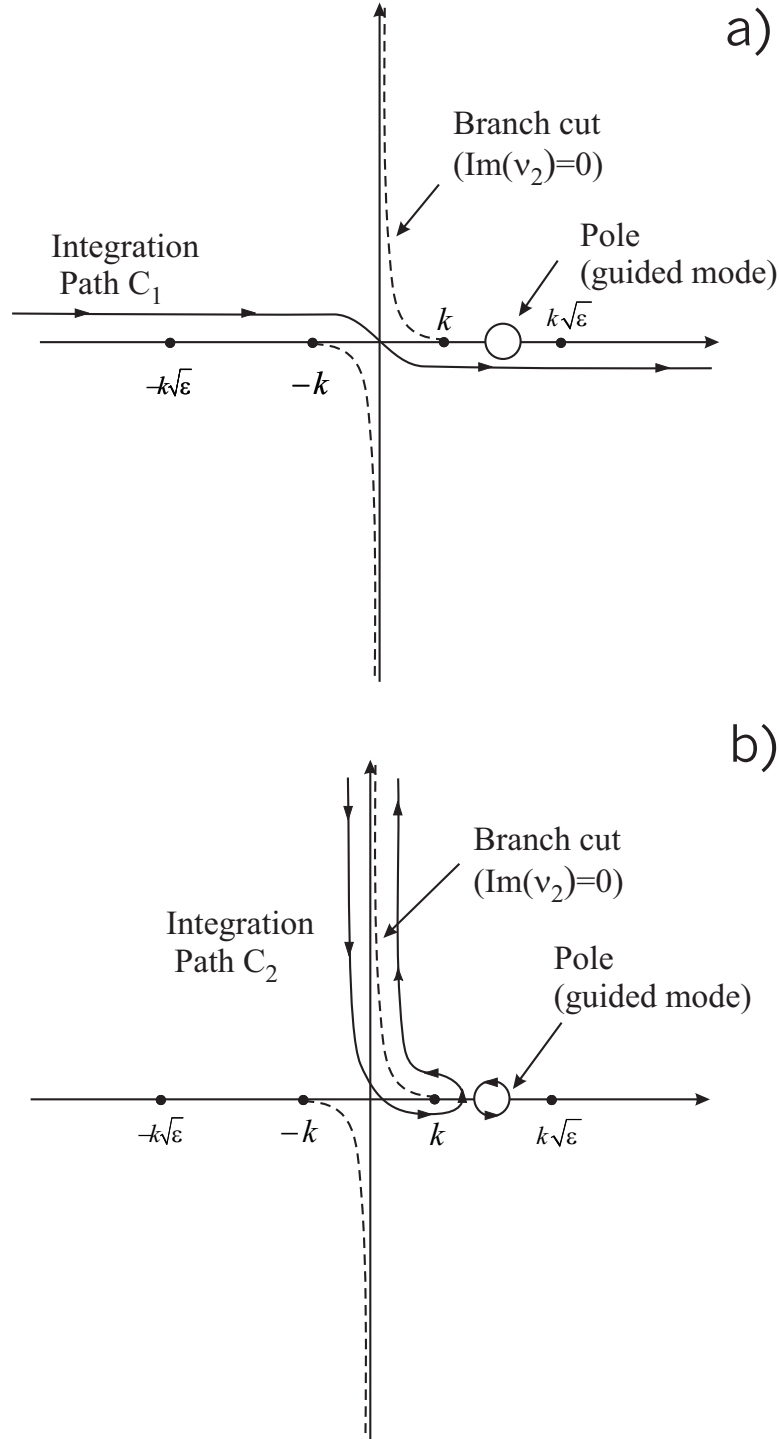


FIG. 2. Integration path for contour integral over longitudinal wavenumber h

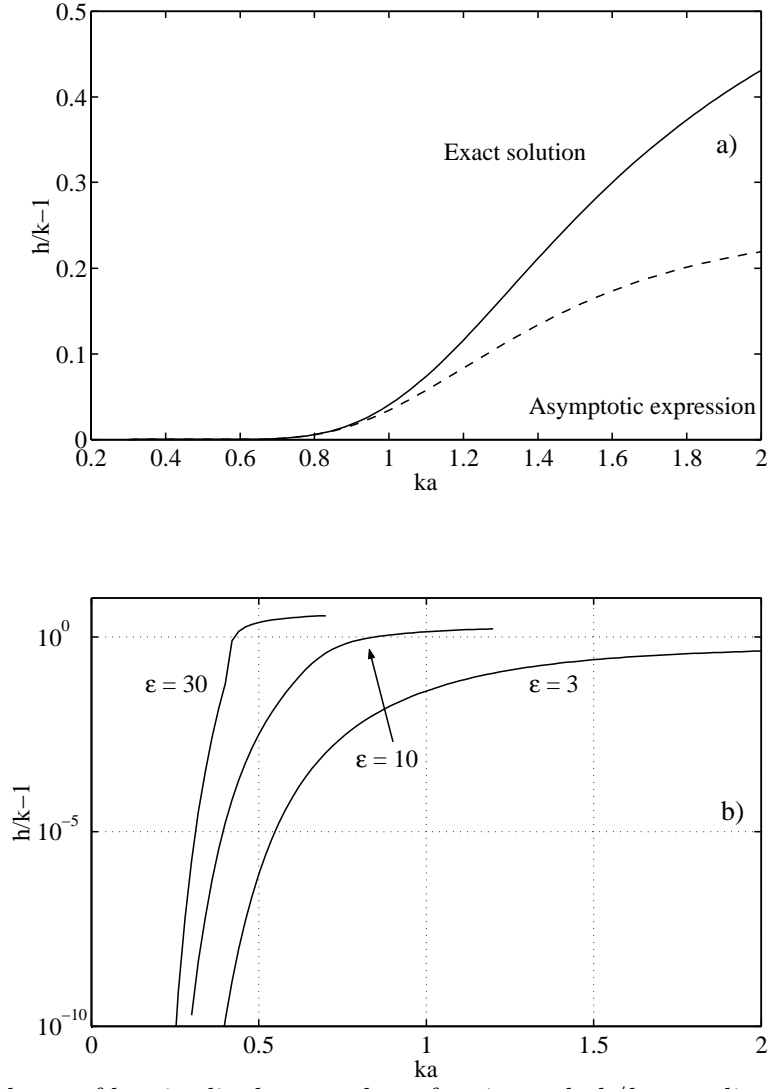


FIG. 3. Dependence of longitudinal wavenumber of main mode h/k on radius of fiber and dielectric constant

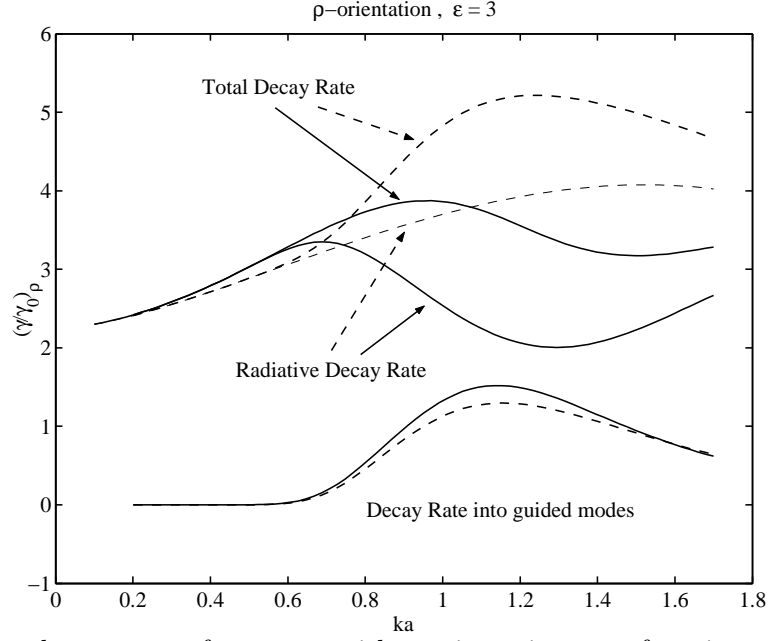


FIG. 4. Relative decay rates of an atom with ρ orientation as a function of radius of fiber ka [Eq.(54), solid lines] and its asymptotic expression [Eq.(56), dashed lines]. (atom on the surface, $\varepsilon = 3$)

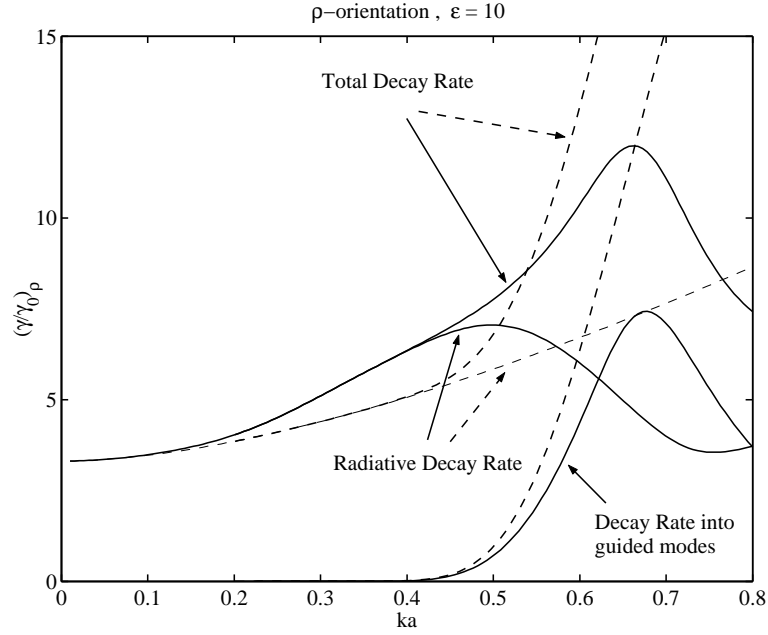


FIG. 5. Relative decay rates of an atom with ρ orientation as a function of radius of fiber ka [Eq.(54), solid lines] and its asymptotic expression [Eq.(56), dashed lines]. (atom on the surface, $\varepsilon = 10$)

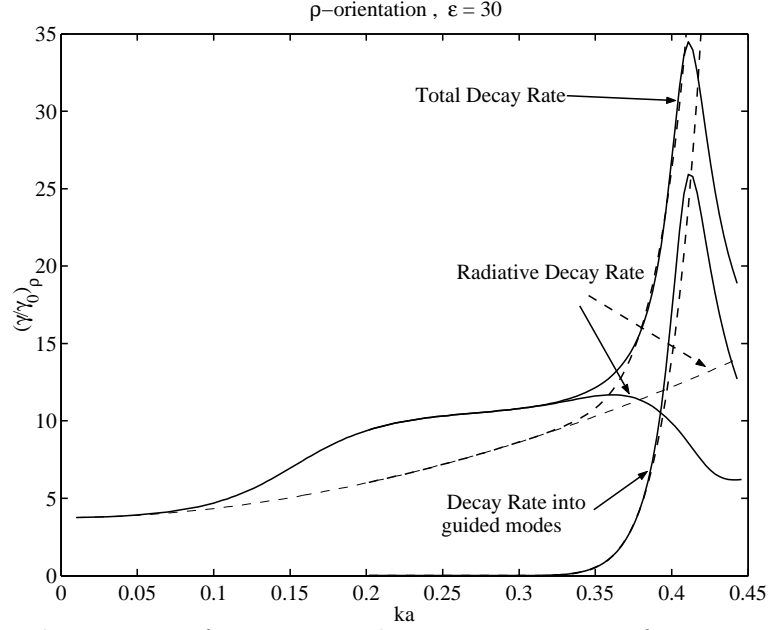


FIG. 6. Relative decay rates of an atom with ρ orientation as a function of radius of fiber ka [Eq.(54), solid lines]) and its asymptotic expression [Eq.(56), dashed lines]. (atom on the surface, $\varepsilon = 30$)

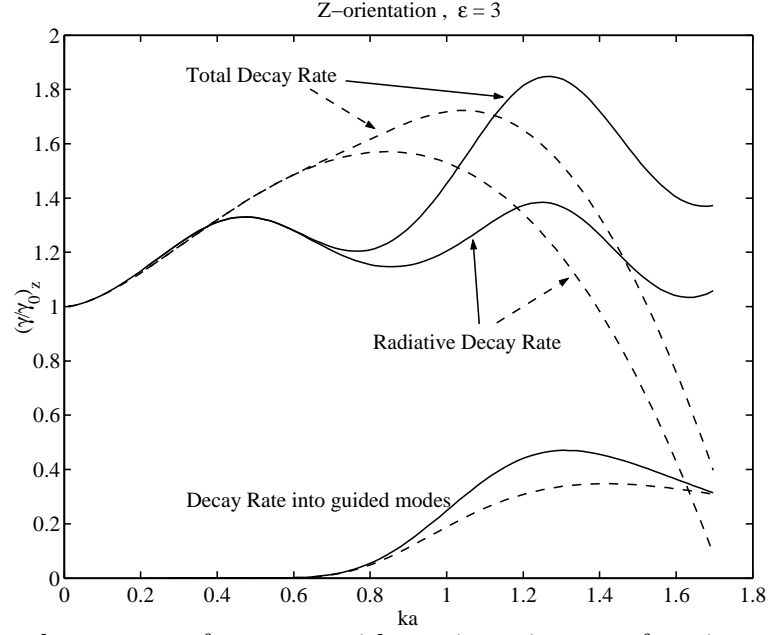


FIG. 7. Relative decay rates of an atom with z orientation as a function of radius of fiber ka [Eq.(48), solid lines]) and its asymptotic expression [Eq.(49), dashed lines]. (atom on the surface, $\varepsilon = 3$)

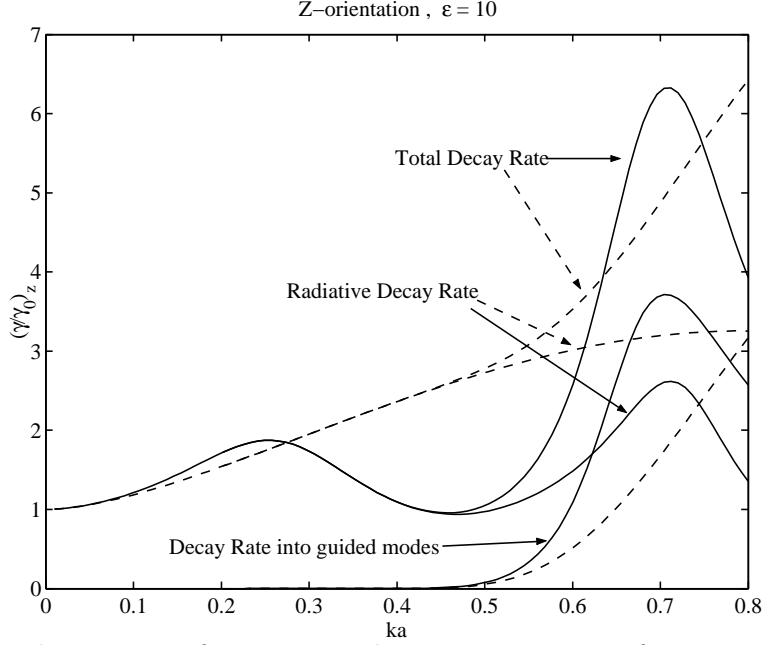


FIG. 8. Relative decay rates of an atom with z orientation as a function of radius of fiber ka [Eq.(48), solid lines]) and its asymptotic expression [Eq.(49), dashed lines]. (atom on the surface, $\varepsilon = 10$)

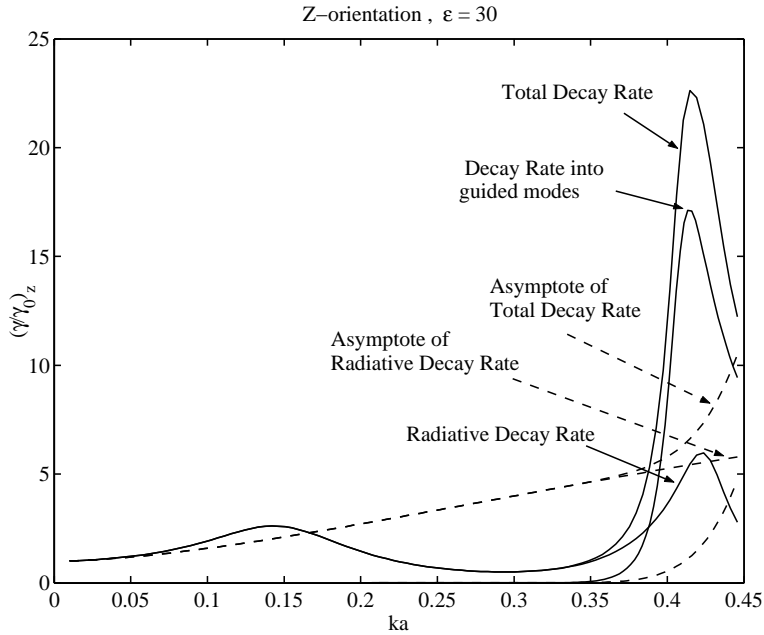


FIG. 9. Relative decay rates of an atom with z orientation as a function of radius of fiber ka [Eq.(48), solid lines]) and its asymptotic expression [Eq.(49), dashed lines]. (atom on the surface, $\varepsilon = 30$)

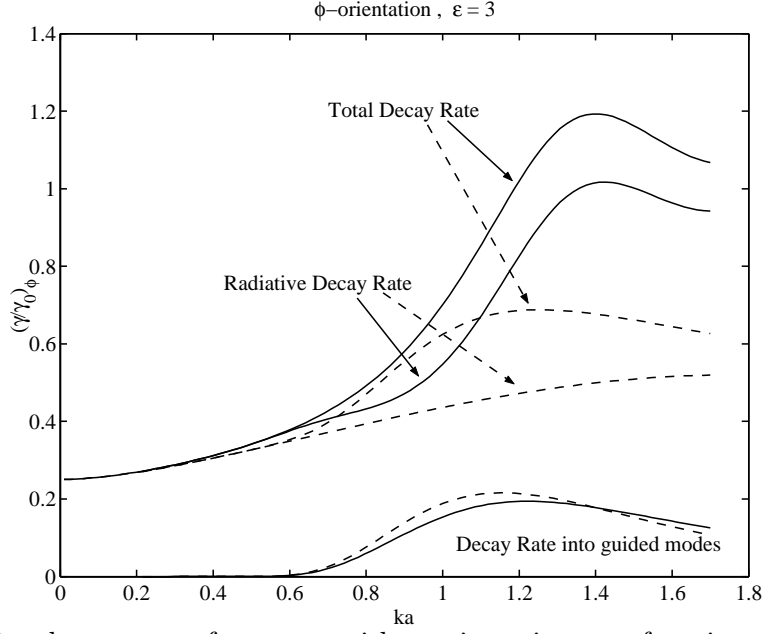


FIG. 10. Relative decay rates of an atom with φ orientation as a function of radius of fiber ka [Eq.(52), solid lines]) and its asymptotic expression [Eq.(53), dashed lines]. (atom on the surface, $\varepsilon = 3$)

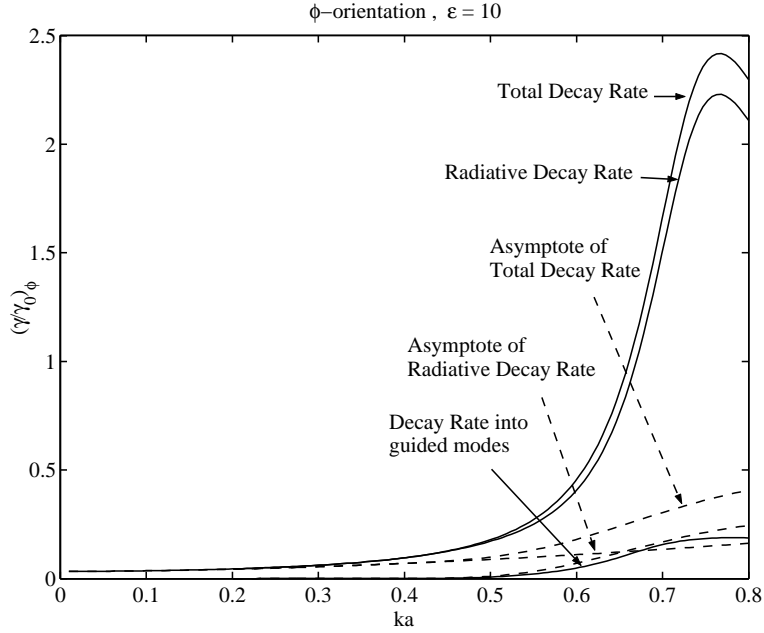


FIG. 11. Relative decay rates of an atom with φ orientation as a function of radius of fiber ka [Eq.(52), solid lines]) and its asymptotic expression [Eq.(53), dashed lines]. (atom on the surface, $\varepsilon = 10$)

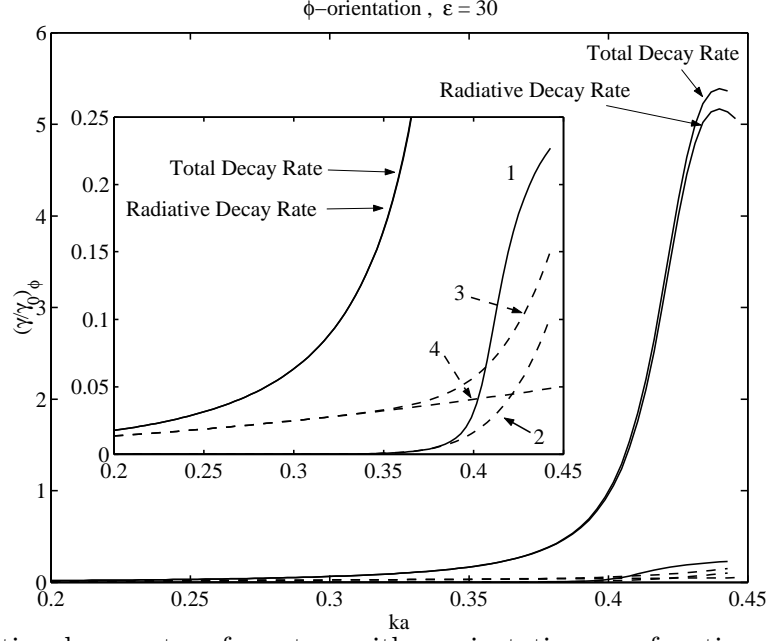


FIG. 12. Relative decay rates of an atom with ϕ orientation as a function of radius of fiber ka [Eq.(52), solid lines] and its asymptotic expression [Eq.(53), dashed lines]. (atom on the surface, $\varepsilon = 30$). On the inset: 1 - decay rate into guided modes, 2 - asymptotic expression of decay rate into guided modes, 3 - asymptotic expression of total decay rate, 3 - asymptotic expression of radiative decay rate

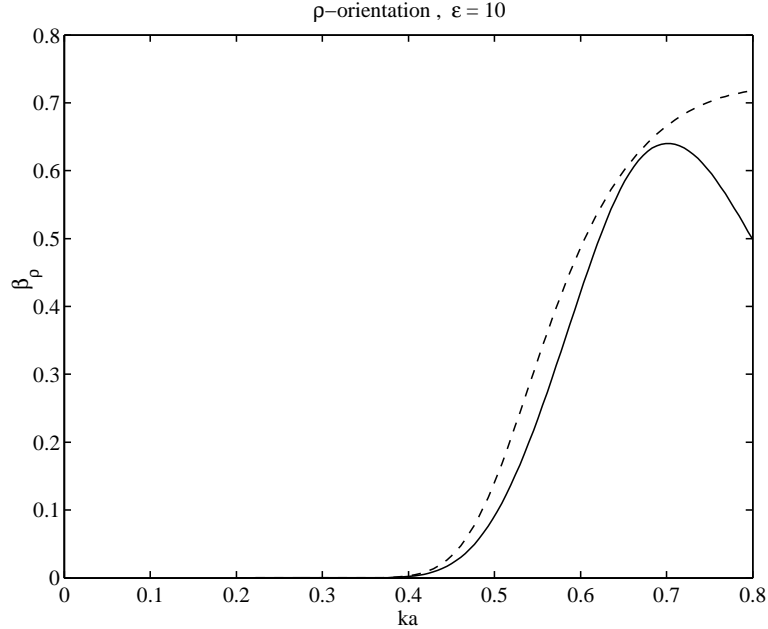


FIG. 13. The spontaneous emission coupling efficiency [Eq.(60)] as a function of radius of fiber ka (solid lines) and its asymptotic expressions (dashed lines) (ρ - orientation, $\varepsilon = 10$)

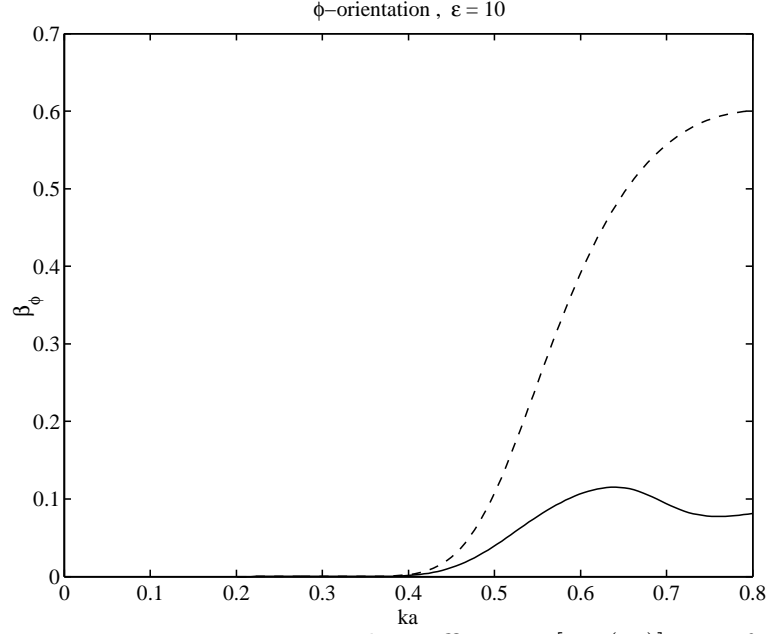


FIG. 14. The spontaneous emission coupling efficiency [Eq.(60)] as a function of radius of fiber ka (solid lines) and its asymptotic expressions (dashed lines) (φ - orientation, $\varepsilon = 10$).

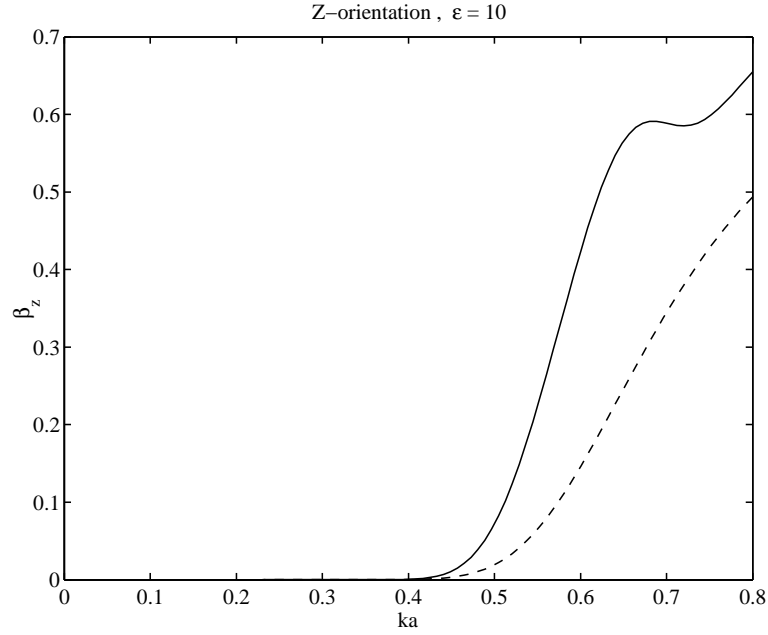


FIG. 15. The spontaneous emission coupling efficiency [Eq.(60)] as a function of radius of fiber ka (solid lines) and its asymptotic expressions (dashed lines) (z - orientation, $\varepsilon = 10$).

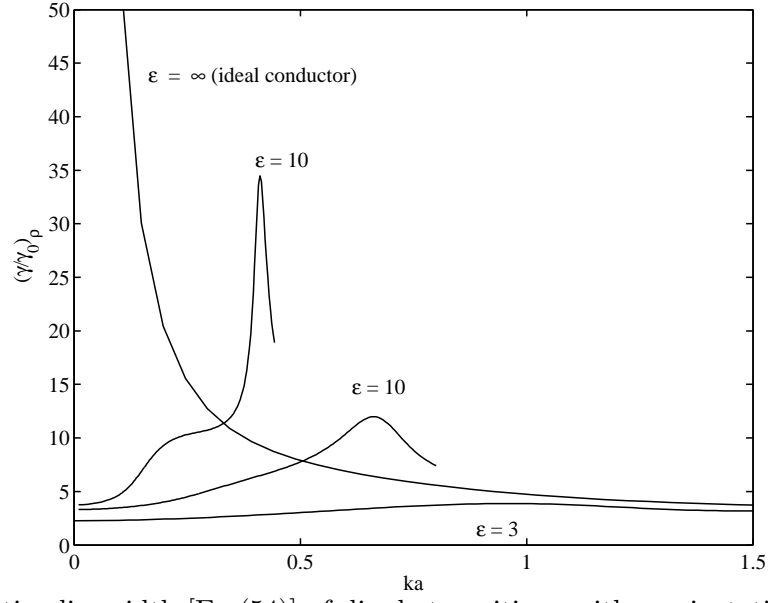


FIG. 16. Relative linewidth [Eq.(54)] of dipole transitions with ρ orientation as a function of fiber radius ka for different $\epsilon = 3, 10, 30$ and for ideally conducting cylinder (atom on the surface).